

**Insights on the role of intermediate waters in the ventilation of the deep-ocean carbon reservoir during the last deglaciation**

Consuelo Martínez-Fontaine<sup>1,3,4</sup>, Ricardo De Pol-Holz<sup>2\*</sup>, Elisabeth Michel<sup>3</sup>, Giuseppe Siani<sup>4</sup>, Dharma Reyes-Macaya<sup>5</sup>, Gema Martínez-Méndez<sup>5</sup>, Tim DeVries<sup>6</sup>, Lowell Stott<sup>7</sup>, John Southon<sup>8</sup>, Mahyar Mohtadi<sup>5</sup> and Dierk Hebbeln<sup>5</sup>

<sup>1</sup>Departamento de Geología, Universidad de Chile; <sup>2</sup>Centro de Investigación GAIA-Antártica (CIGA) and Network for Extreme Environments Research (NEXER), Universidad de Magallanes, Punta Arenas, Chile; <sup>3</sup>Laboratoire des Sciences du Climat et de l'Environnement (LSCE), Laboratoire mixte CNRS-CEA, Avenue de la Terrasse, 91198 Gif-sur-Yvette Cedex, France; <sup>4</sup>Geoscience Paris Sud (GEOPS) Universities of Paris Sud and Paris-Saclay, CNRS, 91405 Orsay, France; <sup>5</sup>MARUM, Center for Marine Environmental Sciences, University of Bremen, Leobener Straße, 28359 Bremen, Germany; <sup>6</sup>Earth Research Institute, UC Santa Barbara, Santa Barbara CA 93106-3060; <sup>7</sup>Department of Earth Sciences, University of Southern California, Los Angeles, California 90089, USA; <sup>8</sup>Earth System Science Department, B321 Croul Hall, University of California, Irvine, California 92697, USA

**Contents of this file**

Figures S1 to S4  
Tables S3 and S4

**Additional Supporting Information**

Captions for Tables S1 to S4

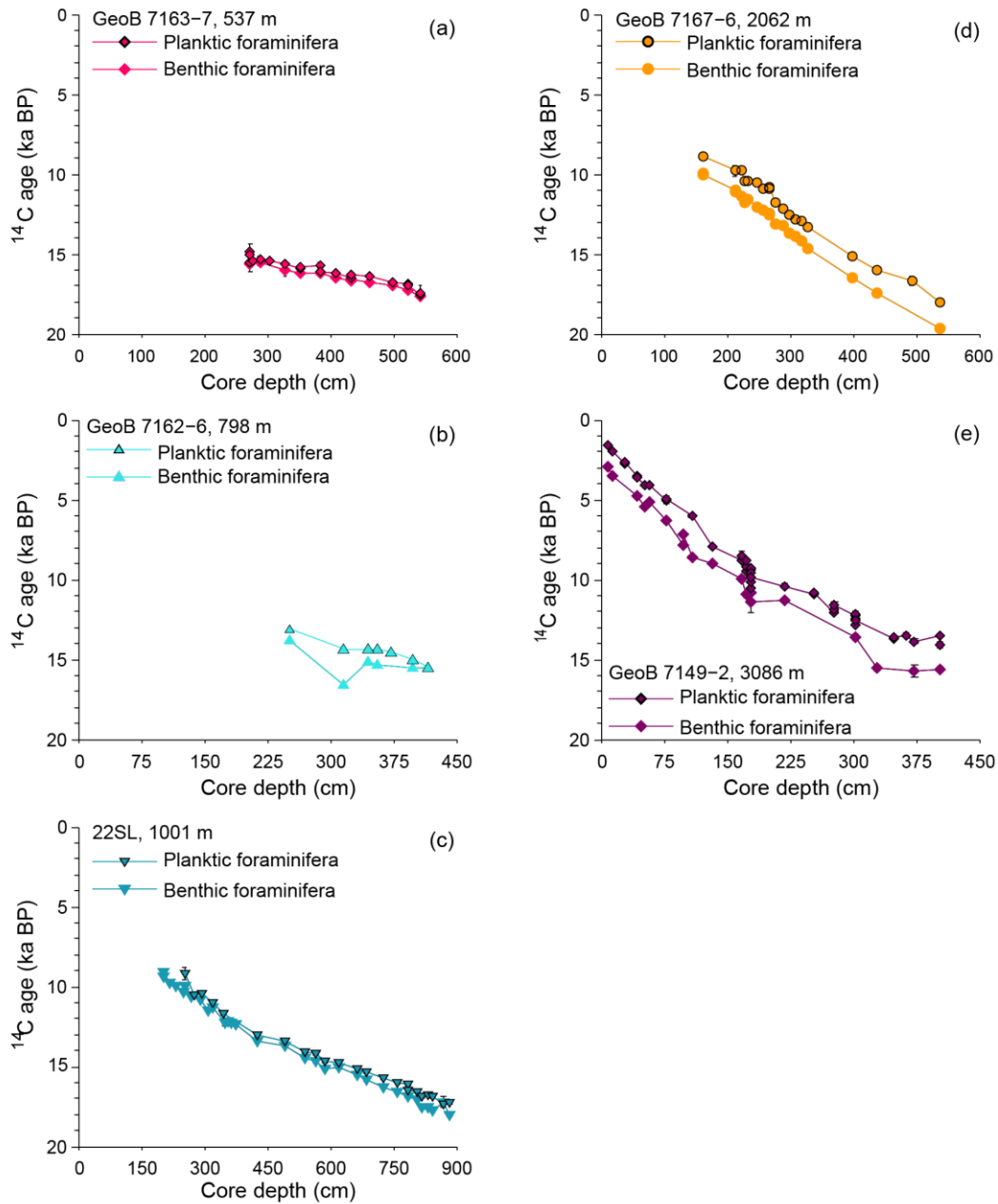


**Figure S1** Planktic and benthic foraminifera conventional (uncalibrated)  $^{14}\text{C}$  ages against core depth. Detailed information in Table S1.

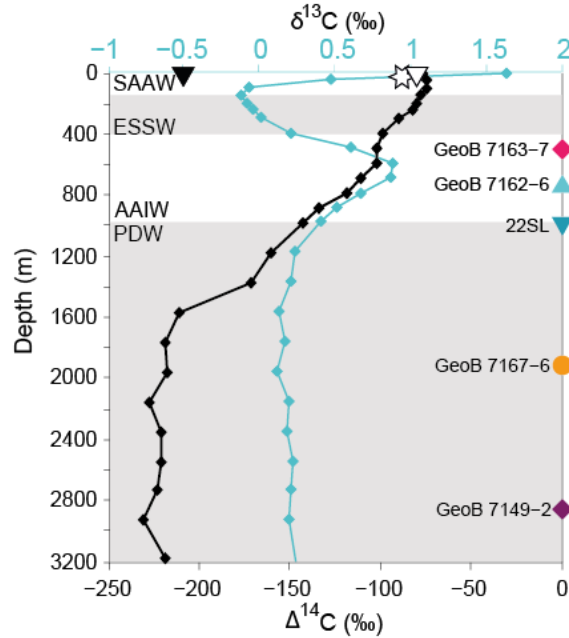


**Figure S2** Modern  $\delta^{13}\text{C}$  (turquoise) and  $\Delta^{14}\text{C}$  (black) water column data from station P06-E11 ( $32^\circ 29.64' \text{ S}$ ,  $72^\circ 42.66' \text{ W}$ ; Kumamoto et al., 2011). For depths shallower than  $\sim 1500 \text{ m}$ , the  $^{14}\text{C}$  corresponds to a natural  $\Delta^{14}\text{C}$  estimate, based on silicate concentrations, alkalinity and apparent oxygen utilization, deeper than  $\sim 1500 \text{ m}$  values are the direct measures. Also indicated in the figure are the mean modern  $\delta^{13}\text{C}$  measured in *G. bulloides* and *N. pachyderma* (dex) in the South East Pacific between  $\sim 24\text{--}46^\circ \text{ S}$  (Mohtadi et al., 2005) and the depth of the studied cores. Black triangle: *G. bulloides* north of  $\sim 35^\circ \text{ S}$ , white triangle: *G. bulloides* south of  $\sim 39^\circ \text{ S}$ ; white star: *N. pachyderma* (dex) between  $\sim 24\text{--}35^\circ \text{ S}$  and  $39\text{--}46^\circ \text{ S}$ . SAAW: Subantarctic Water; ESSW: Equatorial Subsurface Water; AAIW: Antarctic Intermediate Water; PDW: Pacific Deep Water.

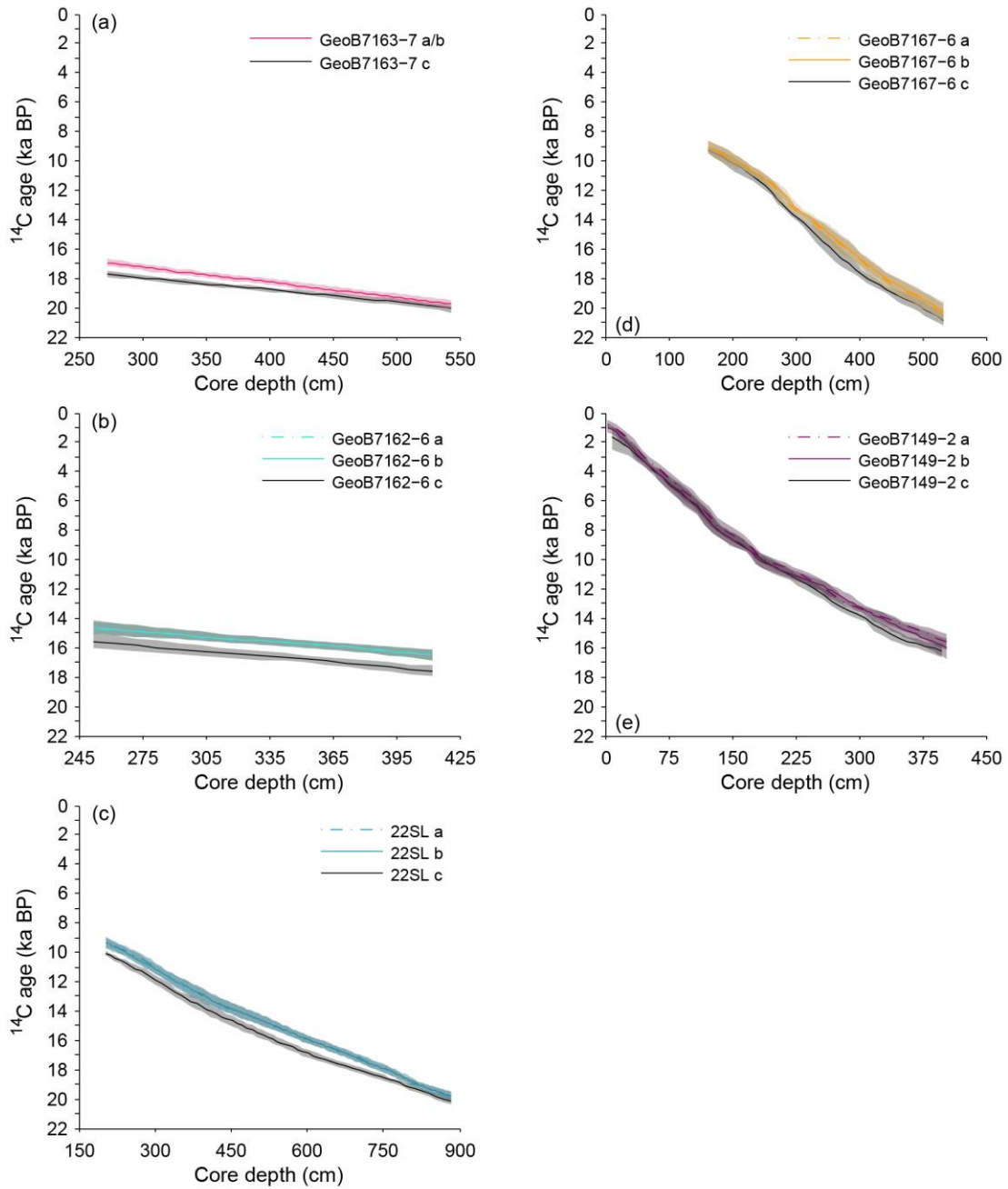


**Figure S3.** Resulting age models for the cores used in this study using the Bacon algorithm (Blaauw & Christen, 2011). The  $R_S$  choice for each scenario is discussed in the main text: a) surface water from SAAW was advected north of  $46^\circ$  S reaching as far north as  $31^\circ$  S throughout all the considered period, and thus the  $R_S$  from core MD07-3088 are applied to all studied cores; b) between  $\sim 13$  and  $\sim 11$   $^{14}\text{C}$  ka BP the upwelling of  $^{14}\text{C}$ -depleted ESSW increases the  $R_S$  at  $\sim 36^\circ$  S (22SL, GeoB 7167-6, GeoB 7162-6) and thus equatorial  $R_S$  from core TR163-23 are assigned for this interval to cores at  $\sim 36^\circ$  S; c) no changes occur in  $R_S$  and thus constant values, equivalent to the modern mean in the closest latitude with available information (Merino-Campos et al., 2019) are

assigned; d) at  $\sim 31^\circ$  S (Geob 7149-2) exclusively equatorial waters flow in the whole interval, and thus for ages older than  $\sim 11$  ka  $^{14}\text{C}$  BP,  $R_S$  from core TR163–23 ( $\sim 0^\circ$  N) are assigned and for ages younger,  $R_S$  ages from  $\sim 32^\circ$  S are assigned (Carré et al., 2015). The colored line corresponds to the weighed mean and its corresponding  $1\sigma$  envelope is plotted, derived from the Bacon.

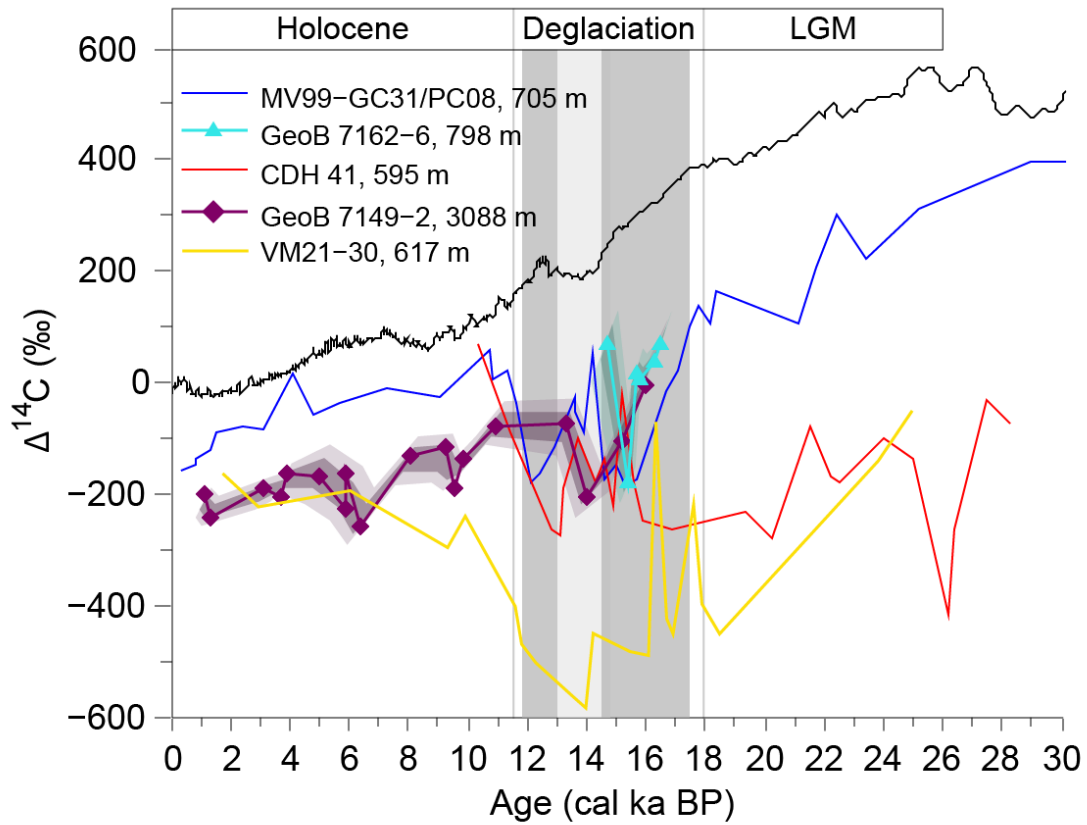


**Figure S4** Comparison of  $\Delta^{14}\text{C}$  in intermediate and deep water from the South East Pacific (this study) with core MV99-MC19/GC31/PC08 in Baja California ( $23.5^\circ$  N,  $111.6^\circ$  W, 705 m; Marchitto et al., 2007) and cores Equatorial East Pacific: CDH 41 ( $1^\circ 15.94'$  S,  $89^\circ 41.88'$  W, 595 m; Bova et al., 2018) and VM21-30 ( $1^\circ 13'$  S,  $89^\circ 41'$  W, Stott et al., 2009). The black curve is the atmospheric  $\Delta^{14}\text{C}$  (Reimer et al., 2013).

**Table S1** Planktic and benthic radiocarbon dates for all cores, calendar and  $\Delta^{14}\text{C}$  obtained according to the text.

**Table S2**  $\delta^{13}\text{C}$  measurements presented in Figure S2. Ages marked with an \* correspond to the original  $^{14}\text{C}$  ages, whereas the rest are the extrapolated ages.

**Table S3** Cores location

Core	Latitude	Longitude	Depth (m)
GeoB 7149-2	31°29.14'S	72°00.00'W	3086
GeoB 7163-7	36°25.54'S	73°35.73'W	537
GeoB 7167-6	36°27.19'S	73°55.50'W	2062
GeoB 7162-6	36°32.52'S	73°40.02'W	798
22SL	36°13.26'S	73°40.50'W	1001

**Table S4** Reservoir ages used in different age models described in the text.

Age model	>13 ka 14C	13-11 ka 14C	<11 ka 14C
a	Rs from MD07-3088	Rs from MD07-3088	Rs from MD07-3088
b	Rs from MD07-3088	Rs from TR163-23	Rs from MD07-3088
c	Rs modern	Rs modern	Rs modern
d (core GeoB 7149-2)	Rs from TR163-23	Rs from TR163-23	Rs from ~32° S
Age model	>13 ka 14C	13-11 ka 14C	<11 ka 14C
a	Rs from MD07-3088	Rs from MD07-3088	Rs from MD07-3088
b	Rs from MD07-3088	Rs from TR163-23	Rs from MD07-3088
c	Rs modern	Rs modern	Rs modern
d (core GeoB 7149-2)	Rs from TR163-23	Rs from TR163-23	Rs from ~32° S